Department of Statistics

UNIVERSITY OF WISCONSIN

Madison, Wisconsin

Technical Report No. 11

August, 1962

DYNAMICS OF AN ADAPTIVE OPTIMIZING CHEMICAL PROCESS

V. Rajaraman

SUMMARY: The dynamic characteristics of the adaptive optimizing chemical process suggested by Box and Chanmugam is obtained by a perturbation solution of the differential equations of the system. It is shown that the adaptive feature of the system can be described by a mathematical model which has the configuration of a simple servomechanism.

This research was supported by the Wisconsin Alumni Research Foundation and the National Science Foundation under contract (NSF-G14768). Reproduction in whole or in part is permitted for any purpose of the United States Government.

Recently a number of schemes for automatically optimizing the performance of chemical processes have been proposed in the literature (6). These range from the use of on-line digital computers to program the optimal values of controllable variables to simple manual feedback as in evolutionary operation (1). For continuous processes, a means of making evolutionary operation automatic has recently been discussed by Box and Chanmugam (2). In order to understand the dynamic behavior of these systems it is necessary to obtain mathematical models describing their self-optimizing feature. Such models provide insight into how the optimizing loop processes the information obtained from the perturbation signals and guides one to the proper choice of the optimizing loop components. The purpose of this paper is to obtain such a model for the adaptive optimizing chemical process discussed by Box and Chanmugam.

Formulation of the problem

The chemical reaction automatically optimized is one in which a reactant N_1 decomposes into N_2 which in turn decomposes into another chemical N_3. It will be assumed that the reaction takes place in an ideally stirred tank reactor into which N_1 is continuously fed in, N_2 is the product of interest and it decomposes into a useless product N_3. In this reaction N_2, called the yield, goes through a maximum as the flow rate X_0 of N_1 is varied. Two other constants k_1 and k_2, called the specific rate constants, influence the process and the reaction may be represented by

$$N_1 \xrightarrow{k_1} N_2 \xrightarrow{k_2} N_3$$

It will also be assumed that the instantaneous rates of decomposition of N_1 and N_2 follow first order kinetics, that is, the rates are proportional to the first powers of the instantaneous concentrations of N_1 and N_2 respectively. The process is automatically optimized by employing a sinusoidal perturbation of the controllable variable (in this case the flow rate X_0) in conjunction with a phase sensitive detector in the optimizing loop which sets the flow rate at its optimum value. The process described above has been discussed in greater detail by Box and Chanmugam (2). The chemical reactor together with the optimizing loop is shown in Figure 1.

The purpose of the optimizing loop may be explained with the aid of Figure 2. In this figure is plotted the yield n_2 as a function of the flow rate X_0 with the rate constant k_2 as a parameter. This constant usually depends on an unmeasurable, uncontrollable variable such as catalyst activity. It is observed that for a fixed k_2 equal to k_{21}, the yield is maximum at the optimum flow rate $X_{opt\ 1}$. The purpose of the optimizing loop is two-fold; a) when k_2 is fixed, it automatically forces the flow rate X_0 to the optimum and maintains it there and b) when k_2 varies with time it continually adjusts the flow rate to optimal values corresponding to the variations of k_2.

The sinusoidal perturbation of the flow rate provides information regarding the state of the process, namely, how far X_0 the actual flow rate is above or below the optimum. This information is processed by the optimizing loop consisting of the detecting multiplier and the integrator and used to automatically set the input flow rate at the optimum value.

One may now pose a number of questions.

1) How does the optimizing loop provide the information for automatically setting the flow rate X_0 at its optimal value?

2) How does the dynamic characteristics of the chemical system affect the performance of the optimizing loop?

3) What are the important parameters that influence the operation of the optimizing loop and how does one find the "best" values of these parameters?

These questions are partially answered by the linearized mathematical model of the optimizing loop derived in this paper.

An analysis of the self-optimizing chemical process

The differential equations representing the sinusoidally perturbed process described in the last section are

$$\frac{dn_1}{dt} = (X_0 + m \cos \nu t)(1-n_1) - k_1 n_1 \quad (1)$$

$$\frac{dn_2}{dt} = k_1 n_1 - k_2 n_2 - (X_0 + m \cos \nu t) n_2 \quad (2)$$

$$\frac{dn_3}{dt} = k_2 n_2 - (X_0 + m \cos \nu t)\, n_3 \quad (3)$$

$$n_1 + n_2 + n_3 = 1 \quad (4)$$

In the above equations $(X_0 + m \cos \nu t)$ represents the sinusoidally perturbed input flow rate; m is the amplitude and ν is the frequency of the perturbation. The yield is n_2 and is therefore the interesting quantity. Equation (3) involves the "waste" n_3 and further there is no coupling back from Equation (3) to

Equation (2); Equation (4) is a constraint relation and thus these equations are not directly useful in the analysis. Therefore, the analysis is limited to the solution of Equations (1) and (2).

The use of block-diagram representation of physical systems in systems analysis needs no overemphasis. This technique was used in analyzing the chemical process discussed in this paper. The block-diagram representing the differential equations of the chemical process and the optimizing loop is shown in Figure (3). [In this section $\rho \cos \lambda t$ and $\sigma \cos \mu t$ in Figure 3 are to be taken equal to zero. These terms are non zero in later sections.] The details of the derivation of the diagram together with an example of how it is used is discussed in the appendix.

It will now be assumed that the optimizing loop is open and the terms at various frequencies comprising n_2 will be determined. This is easily accomplished using the block-diagram (Figure 3) as it clearly indicates the flow of signals in the system. The terms of order m^2 are neglected as they are small compared with the other terms.

1) D.C. term:

$$(n_2)_s = \frac{k_1 X_0}{(X_0+k_1)(X_0+k_2)} + O(m^2) \tag{5}$$

2) Terms at frequency ν:

$$(n_2)_\nu = -\frac{mk_1X_0}{abb_1} \cos(\nu t - \phi_2) - \frac{mk_1X_0}{aa_1b_1} \cos(\nu t - \phi_1 - \phi_2)$$
$$+\frac{mk_1}{a_1b_1} \cos(\nu t - \phi_1 - \phi_2) + O(m^2) \tag{6}$$

where

$$a_1 = [(X_0+k_1)^2 + \nu^2]^{\frac{1}{2}} \quad , \quad b_1 = [(X_0+k_2)^2 + \nu^2]^{\frac{1}{2}}$$
$$a = X_0+k_1 \quad , \quad b = X_0+k_2 \qquad (7)$$
$$\phi_1 = \arctan \nu/a \quad , \quad \phi_2 = \arctan \nu/b$$

The D. C. term represents the steady state yield of the chemical process as a function of X_0 the flow rate, and the specific rate constants k_1 and k_2. When it is differentiated with respect to X_0 one obtains

$$\frac{\partial(n_2)_s}{\partial X_0} = \frac{k_1(k_1k_2 - X_0^2)}{(X_0+k_1)^2(X_0+k_2)^2} \qquad (8)$$

It is seen that $(n_2)_s$ is maximum when $X_0 = (k_1k_2)^{\frac{1}{2}}$. Superposed on the steady value are the varying components due to the introduction of the perturbation at the input; the component at frequency ν being the one useful in the optimization. The varying components are processed by the optimizing loop (lower half of Figure 3) and yield the signal X_f used to alter the input flow rate X_0. The important information regarding the yield and its relation to the input flow rate is furnished by the slope of the process function $\frac{\partial(n_2)_s}{\partial X_0}$. This information is to be extracted by the optimizing loop and used to force the flow rate to its optimum value, namely, to that value which maximises n_2. One method of achieving this would be to adjust the controlled variable(X_0) set point at a rate proportional to $\frac{\partial(n_2)_s}{\partial X_0}$. It will now be demonstrated that the optimizing loop as shown in Figure 3 does this.

Referring to Figure 3 it is assumed that the band pass filter passes the varying components of n_2 freely (i.e. with small phase shift and attenuation) but attenuates the steady (D.C.) component. Thus at its output the important components are the ones given by Equation 6. This output is multiplied by $\cos(\nu t - \psi)$. Keeping in mind that the varying components at the multiplier output are attenuated by the integrator, the useful signal at the output of the detecting multiplier (Figure 3) is given by

$$\begin{aligned}\left[(n_2)_\nu \cos(\nu t - \psi)\right]_{\text{useful}} &= \frac{-m(n_2)_s}{2b_1} \cos(\psi - \phi_2) \\ &\quad + \frac{mk_1^2}{2aa_1b_1} \cos(\psi - \phi_1 - \phi_2) \\ &\approx \frac{dX_f}{dt} \end{aligned} \tag{9}$$

The phase shift ψ used in the above equation is necessary to compensate for the phase shifting of the perturbation signal by the chemical process dynamics. The appropriate value equals $(\phi_1 + \phi_2)$ as may be seen by algebraic manipulation of Equation 9. When this value is used, Equation 9 reduces to

$$\frac{dX_f}{dt} = \frac{mk_1(k_1k_2 - X_0^2)}{(X_0+k_1)^2(X_0+k_2)^2\left[1+\left(\frac{\nu}{X_0+k_1}\right)^2\right]^{\frac{1}{2}}\left[1+\left(\frac{\nu}{X_0+k_2}\right)^2\right]^{\frac{1}{2}}}$$

$$= \frac{\partial(n_2)_s}{\partial X_0}$$

As ϕ_1 and ϕ_2 are functions of X_0, k_1 and k_2, when these change $\psi = \phi_1 + \phi_2$ must be appropriately altered. As pointed out by Box and Chanmugam, it is difficult to do this in practice and one has to be content with a fixed phase shift, chosen

judiciously, which hopefully will not be too different from the ideal value over the range of variation of X_0, k_1 and k_2.

Another quantity worth calculating is the so-called "hunting loss." Referring to Equation 5 it is seen that there is a term of the order m^2. This term arises due to the perturbation and is negative; it consequently reduces the steady state value of the yield. Physically, one may attribute this to the fact that it is necessary to experiment on both sides of the maximum yield to know that one is at a maximum. In large scale chemical processes even a 1% loss is of considerable importance and thus it is necessary to know the parameters that affect this loss. The loss is calculated using the block-diagram (Figure 3) and is

$$L = \frac{m^2 k_1 X_0}{2a_1^2 b_1^2 ab} \left(X_0 \nu^2 + ab^2 + abk_1\right) \tag{11}$$

The effects of varying the amplitude and frequency of the perturbation signal on the loss L is discussed in reference 5.

A linearized mathematical model of the optimizing loop

The self-optimizing system discussed in the last section is non-linear and time varying. Further, the time variations of the system parameters are random. Thus conventional methods of analysis are not promising. One has to understand the basic purpose of the system to be even moderately successful. One of the purposes of the self-optimizing scheme is the estimation of the flow rate variations away from the ideal (i.e. the value giving maximum yield) and its closed loop correction. As soon as this basic aim is understood, one is immediately led to the "black box" representation of Figure 4; this is a conceptual servo, termed

The signal of interest is the "detected" disturbance signal of frequency λ. Thus if the signals at frequencies $\nu \pm \lambda$ at the point 1 are calculated, the useful signal detected at point 2 will be at the frequency λ. Other unwanted frequency components appearing along with the useful signal are termed "measurement noise components," and are displayed as such in the flow rate correction servo.

The useful signal at frequency λ appearing at point 2 of Figure 3 is calculated easily by enumerating the signals at frequencies $(\nu \pm \lambda)$ that appear at 1. (The optimizing loop is assumed open). The "flow graph" of the disturbance signal and the signal components that give rise to these is shown in Figure 5. In this derivation it is assumed that the band pass filter introduces a negligible amount of phase shift at frequencies near ν and that $\nu \gg \lambda$. This implies that the band pass filter has been carefully designed and that the disturbance is much slower when compared with the variations of the perturbation signal,

Thus the open-loop equivalent of the detection scheme employed by the optimizing loop is represented in Figure 5. The detected disturbance signal is fed back to the input flow rate set point in order to provide a closed loop correction for the disturbances. Thus this closed-loop control may be represented by the "Flow Rate Correction Servo" of Figure 6. For slow variations of X_0, not necessarily sinusoidal but restricted to a narrow band of frequencies, the same model is appropriate. If further, the disturbance frequencies are much lower than the reciprocal of the chemical process time constants, the first box in Figure 6 may be replaced by a constant whose value is

$$K = \frac{mk_1}{2a_1b_1}\left[\frac{k_1+b}{a+b} + \frac{a_1^2k_1b + a^2b_1^2}{aa_1^2b_1^2}\right] \qquad (12)$$

It must be recalled that this model is for incremental charges in X_0 about the optimum and the appropriate values of a, b, a_1, b_1 must be used.

The two power spectra $S_m(\omega)$ and $S_n(\omega)$ displayed in Figure 6 represent respectively the measurement noise (discussed earlier), and the noise appearing at the output of the chemical process (due to random noise sources present in the chemical process).

A model to represent rate constant variations

So far, the rate constants k_1 and k_2 were assumed invariant. In practice, they vary in an unknown fashion; the primary purpose of the optimizing loop is to adjust the input flow rate optimally as these constants vary. The dynamic behavior of the optimizing loop in this situation is investigated using the method of the last section. It is assumed that k_2 varies as given by the equation $k_2(t) = (k_{20} + \sigma \cos \mu t)$ and that X_0 is set at the optimum value corresponding to the rate constant values k_1 and k_{20}. If k_2 is assumed constant and k_1 as varying sinusoidally, a dynamic model for variations of k_1 may be obtained.

The block-diagram of the system with sinusoidal variations of k_2 (with the optimizing loop open) is shown in Figure 3 where ρ is set equal to zero as X_0 is assumed undisturbed. The signal at frequency μ appearing at point 2 in that figure is given by $B_1 \sigma \cos \mu t$ where

$$B_1 = \frac{-mk_1^2 b}{a_1 b_1^3 a} \tag{13}$$

The above result is obtained by enumerating the signal components at frequencies ($\nu \pm \mu$) appearing at point 2 of Figure 3 and retaining the terms at frequency μ appearing at the output of the detecting multiplier (multiplier III in Figure 3). When the optimizing loop is closed it is evident from Figure 3 that $\alpha \cos \mu t$ causes a feedback to the input flow rate set point $X_f(t) = \alpha \cos \mu t$. The dynamic model for time variations X_0 was derived in the last section. These two ideas are combined to obtain the mathematical model of Figure 7.

Simulator study of the self-optimized process.

The chemical process discussed in this paper was simulated on a high speed analog computer (with 1 millisecond unit of time) in order to gain insight into its operation, and investigate the validity of the dynamic model of the optimizing loop proposed earlier. The values of the different parameters of the chemical process are (Equations 1 and 2) $k_1 = 0.1\ \text{min}^{-1}$, $k_2 = .05\ \text{min}^{-1}$. A time scale change of $.05t = T$ was used. The frequency of perturbation was 340 cps which is 1000 times larger than if real time simulation had been used. In practice, the flow rate can never be negative and its maximum value will also be limited. An extra loop consisting of a high gain dead zone unit was used to simulate this feature in the computer. The input flow rate (set at the optimum) was sinusoidally disturbed at a low frequency. The gain and phase of the signal detected by the optimizing loop was measured at the output of the integrator in the optimizing loop,

with the loop open and closed. In order to eliminate experimental errors due to measuring instruments, the theoretical model of the optimizing loop (Figure 6) was also simulated on the computer and its open and closed loop gain and phase characteristics were measured using the same instruments. The results are plotted in Figure 8. The continuous curves are for the theoretical model and the individual points are those obtained with the actual system and the agreement is close.

Selecting parameters of the optimizing systems.

As in all engineering problems, there are a number of opposing considerations in choosing the "best" values of the parameters of the optimizing system. The important factors to be taken into account are:

1) Uncertainty in the operation of the optimizing loop due to random noise appearing in the system.
2) Speed of automatic optimization, that is, the speed with which the optimizing loop is able to reset the input flow rate to the optimum value when it is disturbed, and the rapidity with which it is able to track a moving optimum when rate constants vary.
3) The hunting loss discussed earlier.

There is a certain amount of freedom in choosing the following parameters that influence the three factors mentioned above. They are:

1) Amplitude m and frequency ν of the perturbation signal

2) Gain A of the optimizing loop

3) The transfer function of the optimizing loop. In this paper it is assumed to be an integration but it may be advantageous to use a complicated transfer function (3).

Some general comments regarding the choice of these parameters can be made by inspecting the model of the flow rate correction servo. Referring to Figure 6 it is seen that there are two sources of noise in the system. The first source is the random noise present in the system and its spectral density is denoted by $S_n(\omega)$; the second source is due to the unwanted oscillatory terms generated by the perturbation signal and its spectral density is denoted by $S_m(\omega)$. The gain K of the first block in the figure is a function of the perturbation amplitude and frequency. K increases with m and decreases with ν.

A large value of m improves the signal to noise ratio at the output of the system but it increases the hunting loss. A high perturbation frequency also improves the signal to noise ratio by a) dispersing the spectral components of $S_m(\omega)$ and b) shifting the spectrum of $S_n(\omega)$ to $S_n(\omega \pm \nu)$. (If the information bearing signals are confined to low frequencies this shifting of noise spectrum is highly desirable.) This dispersion of spectral components increases the speed of optimization as the flow rate correction servo could be designed to have a higher bandwidth. Practical considerations, however, limit the high values of ν that could be used; the most serious objection being the difficulty

of proper compensation of the large phase shifts at these frequencies.

In this study the controller used in the optimizing loop was assumed to be an integrator. The gain of the integrator A is thus an important parameter to be chosen. The higher the value of A, the larger is the bandwidth of the servo of Figure 6 and thus it is capable of faster operation. The choice of an optimum A depends on the nature of the noise spectrum and the nature of the spectrum of the input signal (namely time variations of X_0, k_1 and k_2). If one can estimate from measurements these spectra, it will be possible to use analytical servo design techniques (4) to find the best value of A. An integrator was assumed to be the controller in this study for simplicity. It might be preferable to use more complicated transfer functions for the controller if the various information and noise spectra are known or postulated (3).

The above discussion shows that the optimization of the optimizing loop parameters is dependent on so many factors that it is an extremely complicated problem. A practical approach seems to be the "design of experiments" on an analog computer to determine the best values of the parameters. The mathematical models derived in this paper provide a basis for an intelligent design of experiments.

Conclusion

The dynamic characteristics of an adaptive optimizing chemical process has been determined using a block-diagram method of analyzing time-varying systems. This method has led to an approximate solution of a complicated problem almost

by inspection. It has been shown that the adaptive feature of the overall system can be described by a simple mathematical model. This model, called the flow rate correction servo, has the configuration of a simple servomechanism with two transfer functions in cascade in its forward path. The first one accounts for the dynamics of the chemical process and the second that of the controller in the optimizing loop. There are two sources of noise which affect the performance of the adaptive optimizer; one of them is the unwanted spectral components introduced due to the perturbation signal and the other the random noise inherent in the chemical process. If enough information about these noise spectra and the nature of time-variation of the chemical process parameters is available, one can use the configuration of the proposed servo model to find the "best" transfer function for the optimizing loop controller.

The flow rate correction servo model for more complicated chemical processes using the Box-Chanmugam optimization technique can easily be obtained using the mathematical method presented in this paper.

APPENDIX

Consider the equation

$$\frac{dn_1}{dt} = (X_0 + m \cos \nu t)(1-n_1) - k_1 n_1 \tag{14}$$

A perturbation technique (7) is used to solve this equation. Rewriting the above equation with the time-varying coefficient on the right (X_0 and k_1 are assumed constant)

$$\frac{dn_1}{dt} + (X_0+k_1)n_1 = m \cos \nu t + X_0 + (m \cos \nu t)n_1 \tag{15}$$

The zeroth order approximate solution is obtained by neglecting the term with the time varying coefficient. (viz. the last term on the right side of Equation 5). Successive solutions are obtained from the recursion equation.

$$\frac{dn_{1\alpha}}{dt} + (k_1+X_0)\, n_{1\alpha} = -m n_{1(\alpha-1)} \cos \nu t \qquad \alpha = 1, 2, 3\ldots \tag{16}$$

The complete solution is the infinite sum

$$n_1(t) = \sum_{\alpha=0}^{\infty} n_{1\alpha}(t) \tag{17}$$

Consider the zeroth order solution. This is obtained by solving the equation

$$\frac{dn_{10}}{dt} + (X_0+k_1)n_{10} = m \cos \nu t + X_0 \tag{18}$$

The solution $n_{10}(t)$ of this equation may be thought of as the output of a linear system described by the transfer function$(1/p + X_0+k_1)$ whose input is $(m \cos \nu t + X_0)$. Referring to Equation (16), the first order solution is obtained

by solving

$$\frac{dn_{11}}{dt} + (X_0+k_1)n_{11} = m_1 n_{10} \cos \nu t \tag{19}$$

This solution $n_{11}(t)$ may again be thought of as the output of a linear system with a transfer function $1/p + (X_0+k_1)$ whose input is $(m_1 \cos \nu t)$ multiplied by the zeroth order solution n_{10} obtained from Equation 18.

Successive solutions are obtained by an entirely analogous technique. This method of solution can be represented pictorially by the block-diagram shown in Figure 9. It is evident that terms higher than the second order have coefficients of power greater than m^2. If the perturbation is small, $m \ll 1$ and these higher order terms may be neglected. Thus in the block-diagram only the first two stages in the solution of the equation need be taken into account.

This block-diagram will now be employed to derive some simple results to demonstrate the use of this approach.

The approximate steady state solution $n_1 \approx n_{10} + n_{11}$ is calculated as follows:

By inspection of the block-diagram

$$n_{10} = \frac{X_0}{X_0+k_1} + \frac{m}{\sqrt{(X_0+k_1)^2+\nu^2}} \cos (\nu t - \phi_1) \tag{20}$$

where the first term is due to X_0 at the input of the system and the second term is due to $m \cos \nu t$ at the input.

Using trigonometric identities

$$-m \cos \nu t \; n_{10} = -\frac{mX_0}{a} \cos \nu t - \frac{m^2}{2a_1} \cos (2\nu t - \phi_1) - \frac{m^2}{a_1} \cos \phi_1 \tag{21}$$

where a, a_1, ϕ_1 are defined in Equation (7).

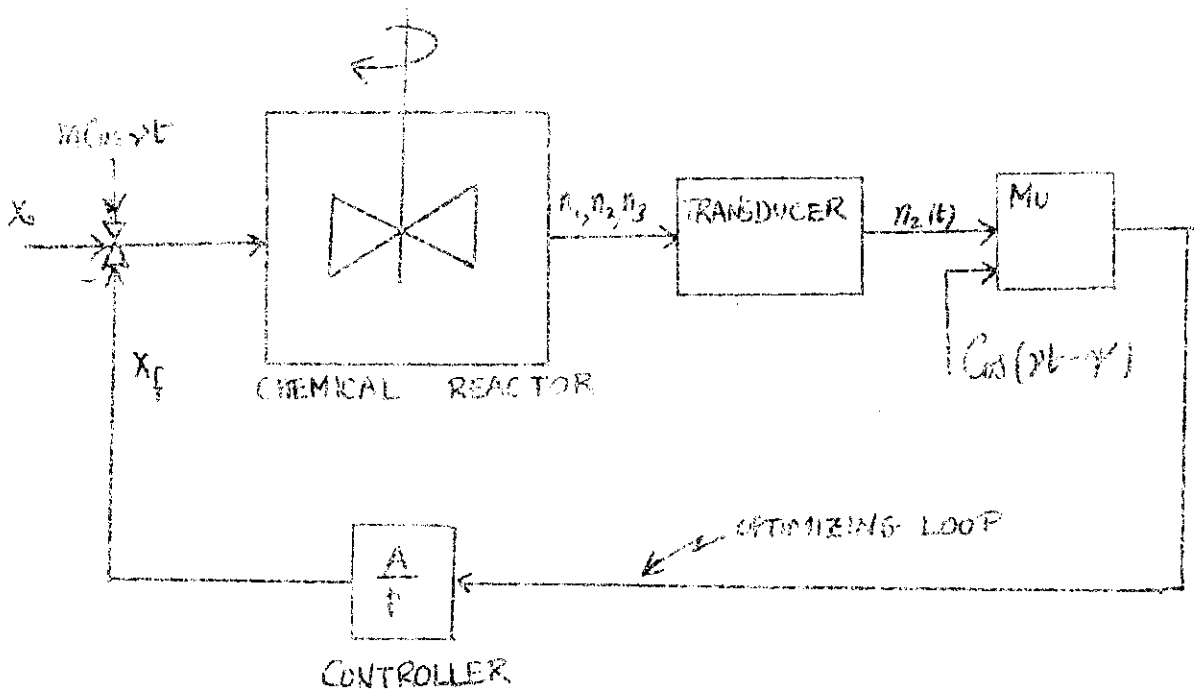

FIG. 1

An adaptive optimizing chemical reactor.

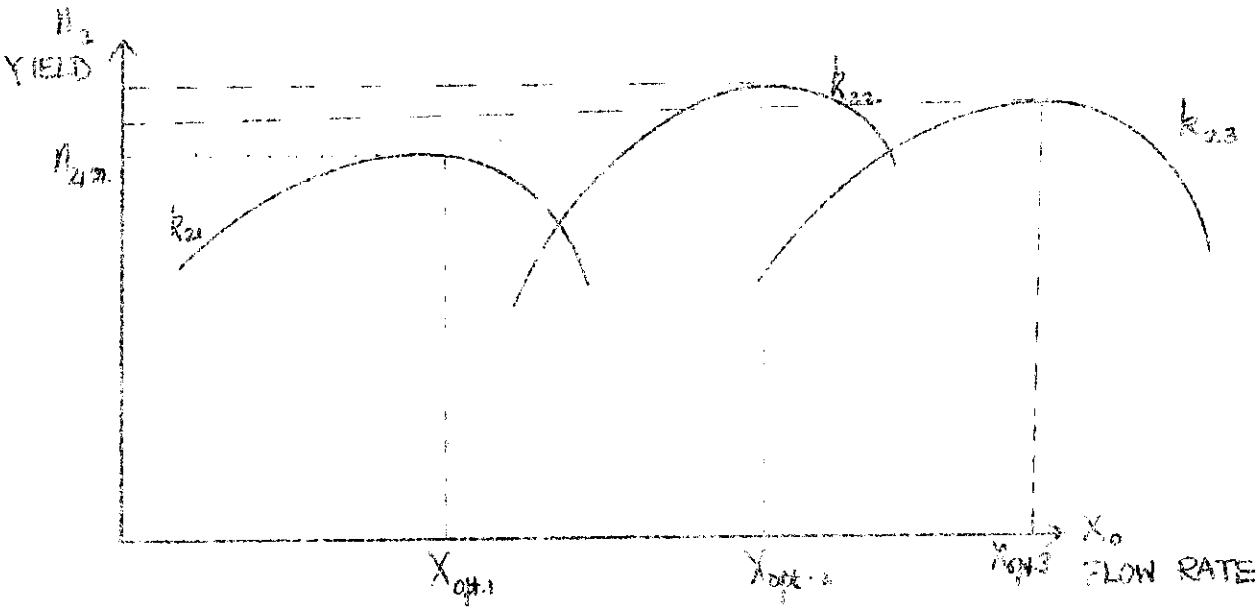

FIG. 2

Steady state process function and its dependence on a nonmeasurable uncontrollable parameter k.

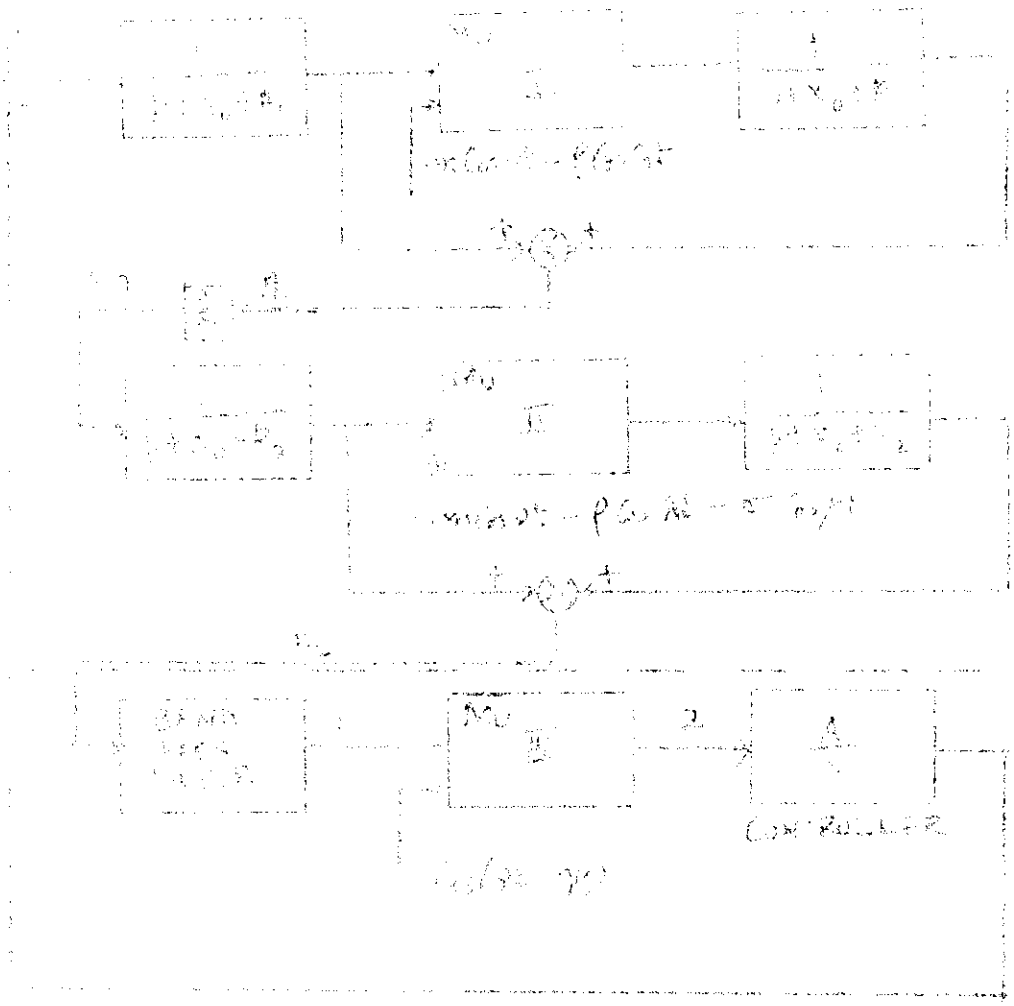

FIG. 3

A block-diagram representation of the chemical process model and the optimizing loop.

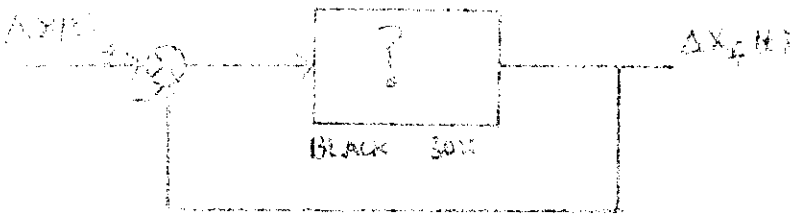

FIG. 4

A servomechanism model to explain the automatic correction of flow rate.

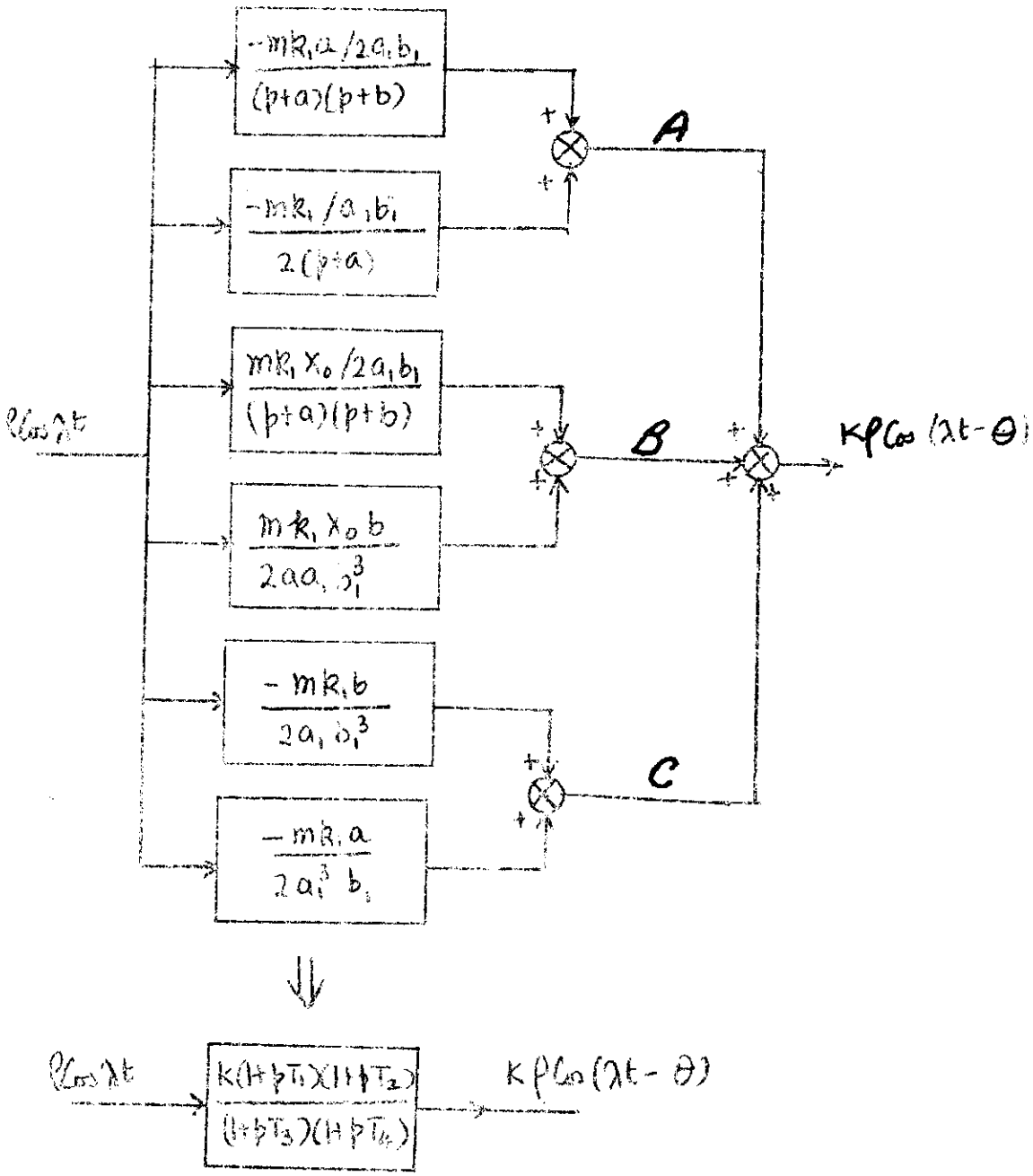

FIG. 5

Model representing dynamics of the chemical reactor for changes in flow rate. The signal at point A of the figure is due to the multiplication of Cos λt at the input by Cos νt in the system, the one at B due to X_0 at input and Cos νt and Cos λt in the system and that at C due to Cos νt at input and Cos λt in the system.

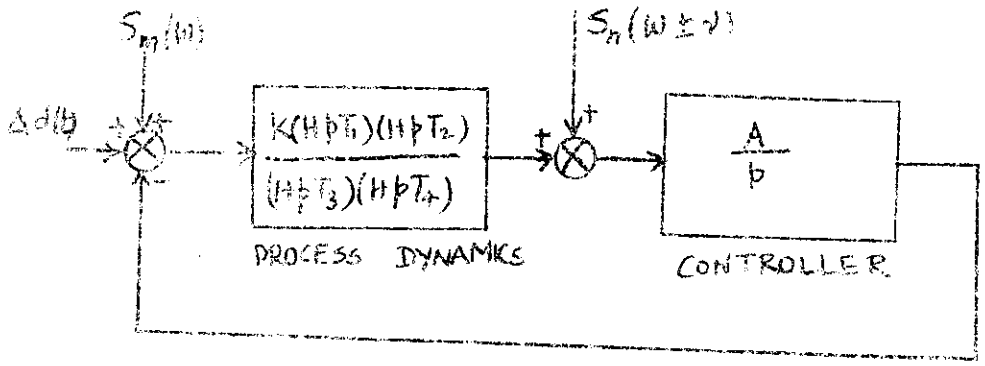

FIG. 6

The model for the flow-rate correction servo.

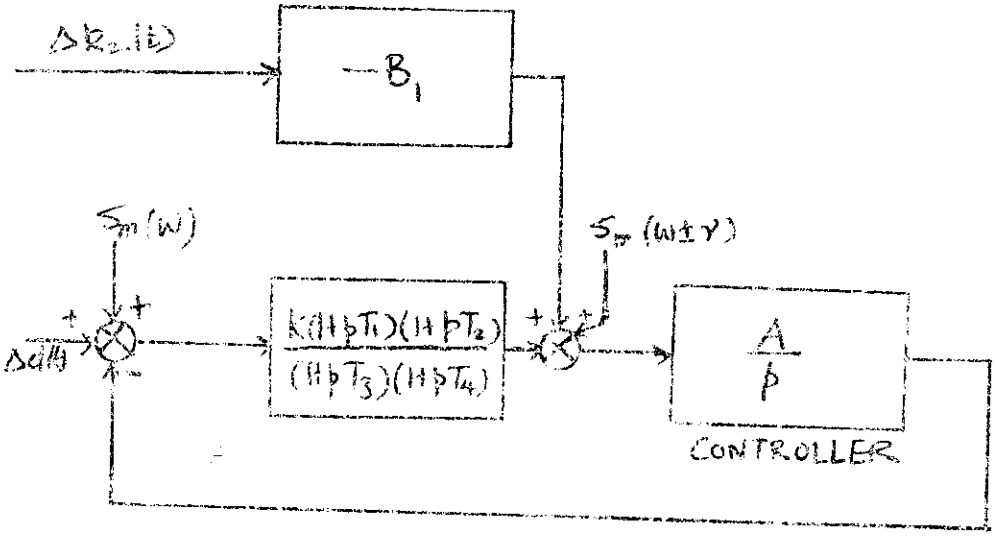

FIG. 7

Model which accounts of changes in flow rate as well as the rate constant.

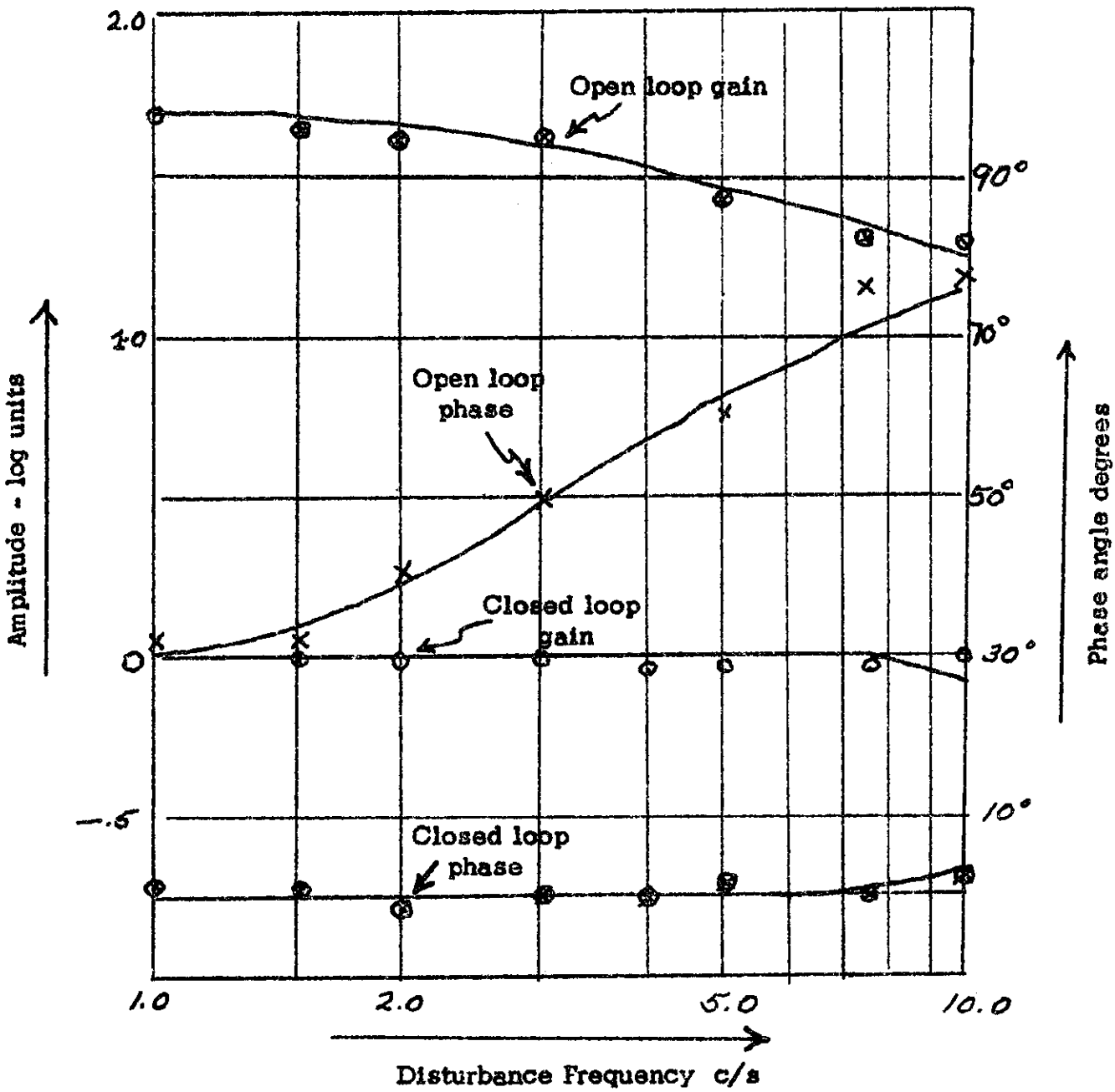

FIG. 8

Curves demonstrating the validity of the flow rate correction servo model.

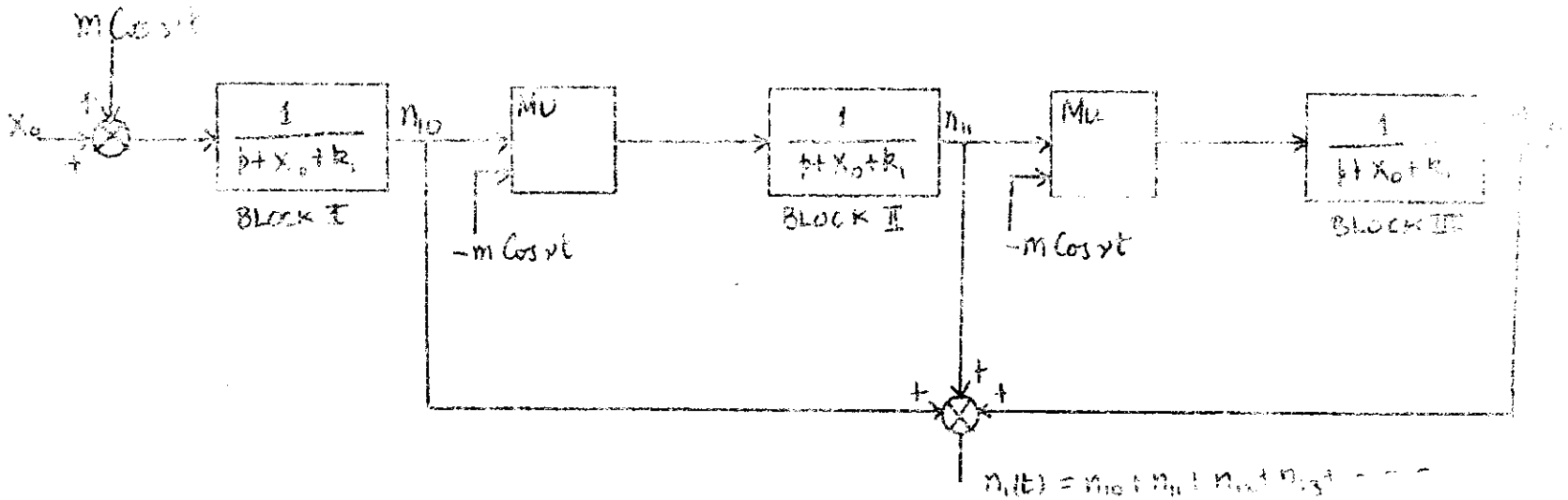

FIG. 9.

Illustrating the block-diagram method of solution of the differential equation with time-varying coefficients.

REFERENCES

[1] Box, G. E. P., Applied Statistics, 6, 3, (1957).

[2] Box, G. E. P. and Chanmugam, J., I and EC Fundamentals, 1, 2, (1962).

[3] Box, G. E. P. and Jenkins, G. M., J. Roy. Stat. Soc., Series B, April 1962.

[4] Newton, G. C., Gould, L. A., Kaiser, J. F., "Analytical design of feedback control systems", John Wiley and Sons, New York, 1957.

[5] Rajaraman, V., Ph. D. Thesis, University of Wisconsin, Madison, Wis., June 1961.

[6] Rideout, V. C., Rajaraman, V. and Benedict, T. R., "A Digest of Adaptive Systems," Cornell Aeronautical Laboratories Rpt. #ID-1384-P-2, March 1962.

[7] Zadeh, L. A., Proceedings Institute of Radio Engineers, (U. S. A.), 38, 291, (1950).

ACKNOWLEDGEMENT

The author expresses his appreciation to Professors Vincent C. Rideout and George E. P. Box for many discussions relating to this paper.